Mechanistic insights into lysine-targeting covalent inhibition through a theoretical study of ester aminolysis

Volkan Findik, Manuel F. Ruiz-Lopez, Safiye Sağ Erdem

Organic & Biomolecular Chemistry

Accepted Manuscript

This article can be cited before page numbers have been issued, to do this please use: V. Fndk, S. S. Erdem and M. F. Ruiz-López, *Org. Biomol. Chem.*, 2021, DOI: 10.1039/D1OB01963E.

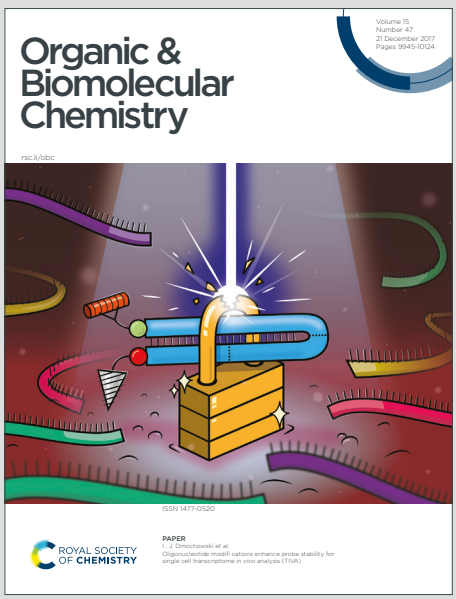

ROYAL SOCIETY OF CHEMISTRY

rsc.li/obc

View Article Online
DOI: 10.1039/D1OB01963E

ARTICLE

Mechanistic insights into lysine-targeting covalent inhibition through a theoretical study of ester aminolysis

Received 00th January 20xx,
Accepted 00th January 20xx

DOI: 10.1039/x0xx00000x

Volkan Fındık[a,b], Manuel F. Ruiz-López*[a] and Safiye Sag Erdem*[b]

Development of targeted covalent inhibitors in drug design has a broad and important interest and many efforts are currently being made in this direction. Targeted covalent inhibitors have special relevance in oncology due to the possibilities they offer to overcome the problems of acquired resistance. In recent experiments, lysine-targeting has been envisaged for the irreversible inhibition of the heterodimeric lipid kinase phosphoinositide 3-kinase delta (PI3Kδ). Activated esters have been evaluated and shown to be promising inhibitors of this enzyme, but the reaction mechanisms display specificities that are not yet fully understood. In the present work, we have carried out a theoretical study of the aminolysis reaction of model esters in aqueous solution to gain insights into the corresponding biological processes. We have found that phenolic esters bearing electron-withdrawing groups are particularly reactive. The predicted mechanism involves the formation of a tetrahedral zwitterionic intermediate, which dissociates into an alkoxide and a protonated amide, this charge separation being the driving force for the subsequent proton transfer and final product formation. Structure-reactivity relationships are reported and shown to be a useful tool for evaluating potential inhibitor candidates.

Introduction

Chemical reactions leading to the formation of amide bonds are of paramount importance in synthetic organic chemistry, polymer chemistry, prebiotic chemistry, biochemistry, or drug discovery.[1–8] In this regard, one of the most interesting reactions is the aminolysis of esters (reaction 1), which allows generating the amide functional group in a wide range of domains, going from material synthesis to biosynthetic routes.[8–11] When the acetyl group is involved (R^1=-CH_3), the reaction is also called N-acetylation, and in proteins it may occur either on N-terminal aminoacids or on internal lysine residues. The first process is typically catalyzed by N-terminal acetyltransferases,[12] while the second is usually catalyzed by lysine acetyltransferases, but can also proceed non-catalytically.[13]

$$R^1COOR^2 + R^3NH_2 \rightarrow R^1CONHR^3 + R^2OH \quad (1)$$

Covalent conjugation with lysine residues in proteins through reaction (1) has recently received attention as a potential process for developing targeted covalent inhibitors (TCIs) in drug design. Indeed, the use of TCIs represents an extremely promising approach in medicinal chemistry[14–19] especially after the emergence of new methods that allow minimizing the risks related to possible toxicological issues.[14] TCIs have attracted a lot of interest in oncology because of the ability to circumvent problems of acquired resistance. Inhibitors targeting cysteine residues in kinases have principally been investigated,[14–16,20–26] but due to limited applicability with human kinases, lysine-targeting covalent inhibitors have been explored as a possible alternative with encouraging results. [27]

Though targeting covalent combination with lysine is challenging owing to the usual protonation state of this residue at physiological pH, Dalton et al[28] have demonstrated the feasibility of the approach. The authors have investigated the kinome-conserved lysine as a possible target for the selective and irreversible inhibition of the heterodimeric lipid kinase phosphoinositide 3-kinase delta (PI3Kδ). A number of selective reversible inhibitors for this enzyme are already used in clinical trials for the treatment of relapsed follicular B-cell non-Hodgkin lymphoma, or relapsed chronic lymphocytic leukemia,[25,26,28–31] but covalent inhibition opens new perspectives. Based on previous works aiming at optimizing indazole inhibitors of PI3Kδ for the treatment of respiratory diseases,[31] Dalton et al[28] have proposed the use of activated esters as electrophiles, and have conducted a kinetics study comparing the phenolic esters shown in Scheme 1.

[a] LPCT, UMR 7019, University of Lorraine, CNRS, 54000 Nancy, France. E-mail: Manuel.Ruiz@univ-lorraine.fr
[b] Department of Chemistry, Faculty of Arts and Sciences, Marmara University, 34722 Istanbul, Turkey. E-mail: erdem@marmara.edu.tr

Electronic Supplementary Information (ESI) available: Coordinates and energetics of all the structures described in the manuscript. See DOI: 10.1039/x0xx00000x

View Article Online
DOI: 10.1039/D1OB01963F

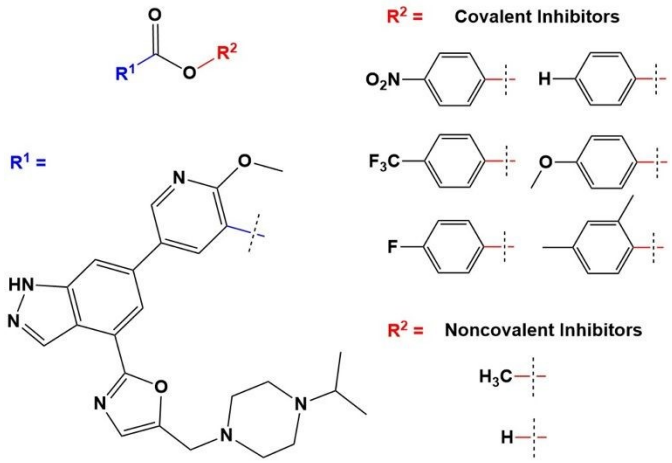

Scheme 1 Potential inhibitors of the PI3Kδ enzyme considered in biochemical and cellular assays by Dalton et al[28] (adapted from Table 1 of their paper).

From their results, the multi-step mechanism indicated in Figure 1 has been proposed, which is slightly more complicated than the traditional two-steps mechanism for TCI. The first step consists of the usual reversible, non–covalent binding of the inhibitor to the enzyme active site. Then, the ester adds to the kinase Lys779 forming a covalent tetrahedral zwitterionic intermediate. This reaction step, assumed also to be reversible, is expected to be affected by the nature (e.g. pK_a) of the leaving phenolic alcohol. The subsequent two steps involve 1) proton loss to form an anionic unstable intermediate, assumed to be the rate determining step, and 2) irreversible, fast breakdown of this intermediate to form the products. The measured K_I has been found to depend on the leaving group, while the measured k_{inact} has been shown to be little affected by the nature of the ester. The authors concluded that K_I encompasses the first two steps, while k_{inact} combines the last two.

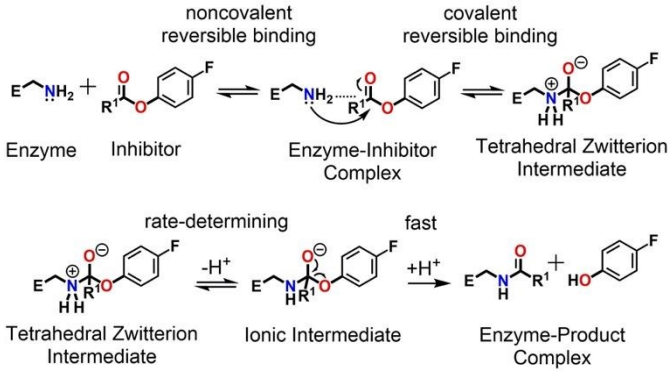

Figure 1. Reaction mechanism proposed by Dalton et al[28] for the covalent inhibition of PI3Kδ targeting Lys779 (adapted from Scheme S1 of their paper) illustrated in the case of a 4-fluoro phenyl ester. The measured K_I was assumed to encompass the first two steps (top) and k_{inact} the last two steps (bottom).

Obtaining a more in depth understanding of the underlying biochemical mechanism is an important goal that can help optimizing the inhibitor efficiency. In this respect, advanced molecular modeling techniques represent a unique tool to elucidate the microscopic details of the reaction mechanism, and the combination of theoretical calculations with experimental kinetic data should certainly be key for rapid progress in the field. The mechanism of amide bond formation through ester aminolysis, reaction (1), has been the subject of many theoretical studies in the past using different models and approaches, and possible pathways have been analyzed.[32–45] However, the mechanism of the aminolysis of activated esters in aqueous solution is not yet fully understood, despite some experimental studies.[46–51] Some theoretical calculations are available in acetonitrile solution,[35,41,42] but the reaction mechanism is arguably different in this case since the formation of zwitterionic intermediates was ruled out under these conditions, whereas such process is expected to play a central role in aqueous solution. However, modeling in aqueous environment is more challenging and complicated because of the handicaps in theoretical characterization of the zwitterionic and ion-pair species.

In the present work, our aim is to get a deeper insight into the reaction mechanism of the aminolysis of PI3Kδ inhibitors (Scheme 1) in aqueous solution, since Lys779 (the residue targeted by the inhibitors) is located near the water accessible surface.[28] Though the reaction in water is expected to present variations with respect to the reaction in the PI3Kδ enzyme, the qualitative trends found for the series of ester derivatives should provide useful insights into the important factors that govern the inhibition process. We first study the reaction mechanism of some model systems, namely, methylamine (CH_3NH_2) with phenyl acetate (PA) and 4-nitrophenyl acetate (or *p*-nitrophenyl acetate PNPA). Methyl acetate (MA) has also been considered for comparison, and as a reference to evaluate the efficiency of phenyl derivatives, as done in PI3Kδ experiments.[28] We assume a combined discrete-continuum model for the water solvent similar to that used before by Gorb et al[52] for a related fundamental reaction (formamide hydrolysis), which reported results in excellent agreement with experimental kinetics data. Similar models have been used by other authors for other aminolysis processes.[38,39,44,53,54] We will then analyze the results in terms of the electronic properties of the leaving group trying to get some qualitative correlation with the experimental data for the series of model esters summarized in Scheme 2. Finally, the potential implications of our results for the improvement of inhibitor efficiency will be discussed.

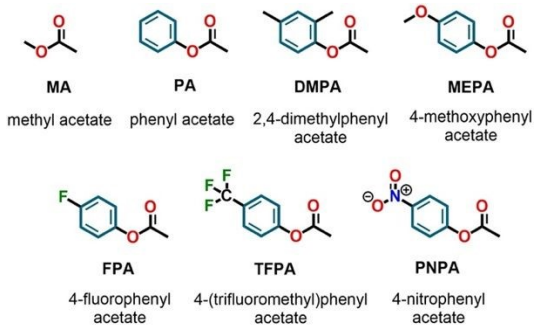

Scheme 2. Model ester derivatives considered in our study.

View Article Online
DOI: 10.1039/D1OB01963E

2. Computational methods

In our study, we have considered a combined explicit-implicit, or discrete-continuum solvation model. Specifically, we have included five explicit water molecules in the chemical system, and we use the polarizable continuum solvation model (PCM, assuming the static dielectric constant of water) to account for long-range solvation effects. The explicit-implicit solvation model has been chosen after some preliminary test computations and is similar to that used in related previous studies[52]. The inclusion of explicit water molecules is compulsory to correctly describe the mechanisms involving zwitterionic and charged species. Previous studies have shown that when a pure continuum solvation model is used, only neutral species based mechanisms are found,[41,45,55] and the same applies for explicit-implicit models using a very small number of explicit waters (see for instance Yang et al.[38]). Some detailed studies on zwitterion stability as a function of explicit water molecules number have been reported.[39] Explicit consideration of five water molecules appears to be a good compromise between accuracy and computational cost.[44] In our computations, the initial position of the water molecules has been chosen based on the most plausible locations to form hydrogen-bonds with the reactants, as well as using data reported in previous studies for related systems.[39,44,56] In most cases, we have explored different orientations, in particular to describe proton transfer elementary steps. In these cases, the possibility for direct and water assisted reactions has been contemplated.

Geometry optimizations, frequency and intrinsic reaction coordinate[57] (IRC) calculations have been performed by means of density functional theory (DFT) based methods at B3LYP[58]/6-311+G(d,p) level of theory. Electronic energies have been improved through single-point energy computations at the MP2[59]/aug-cc-pVTZ levels on B3LYP/6-311+G(d,p) optimized geometries. Zero-point energy and thermal contributions calculated at the B3LYP/6-311+G(d,p) level where then added to these refined electronic energies to obtain total free energies (we assume a reference state 1M at T=298K). The nature of the stationary points, minima or transition structures (TS), was checked by a frequency analysis (zero or one imaginary frequency, respectively). The minima joined by each transition structure were determined through the IRC computations followed by full geometry optimization.

Our solvation model does not allow describing proton transfers to bulk water in detail since we use an implicit model for long-range interactions. The relative energy of the process can be estimated by using the experimental free energy of the hydrated proton, as described in the supporting information of Ref[60] ($G_{aq}(H^+)$ = -270.28 kcal/mol, reference state 1M). In addition, we have computed the free energy profile for the explicit proton transfer to water molecules in the first shell, forming a tetrahedral ion pair $T^-...(H_3O)^+$, which can be considered to be the first step in the proton transfer to the bulk water solvent.

Electrophilicity indices ω for the various ester molecules have been calculated at the B3LYP/6-311+G(d,p) level in gas phase as:[61]

$$\omega = \frac{\mu^2}{\eta} \quad (2)$$

where the chemical potential μ, and the chemical hardness, η, are approximated given as:

$$\mu = \frac{1}{2}(\varepsilon_{HOMO} + \varepsilon_{LUMO}) \quad (3)$$

$$\eta = (\varepsilon_{LUMO} - \varepsilon_{HOMO}) \quad (4)$$

All calculations have been carried out by Gaussian09 software package.[62] The default integration grid for DFT-based computations in Gaussian 09 (fine grid) has been used.

3. Results and discussion

We first present and discuss in detail the mechanisms for the reaction of methylamine with MA, PA, and PNPA esters. We have explored the potential energy surface trying to locate all the relevant stationary points to determine the possible pathways. These calculations have been guided by the results of previous studies on different esters[34,35,45,47,48,63,64]. The different pathways found are shown in Figure 2. The nomenclature used thorough the paper for the different species is defined in the Figure caption.

All mechanisms start by the formation of a non-covalent reactant complex (RC), which then evolves to the characteristic covalent tetrahedral intermediate exhibiting a zwitterionic structure, $T^{\pm}$ (Figure 2a). This $T^{\pm}$ species results from the formation of a covalent bond between the N atom of the amine and the C atom of the ester COO group. We have also explored the potential energy surface corresponding to a direct addition of the amine N-H group to the ester C=O or C-OR bonds, leading respectively to the formation of a neutral tetrahedral intermediate or the final products, but the computations for the three esters considered failed to locate any transition states for these hypothetical reaction pathways. From $T^{\pm}$, four main mechanisms (A-D) have been found, with some variants and specificities depending on ester derivative, as described in detail below. Figure 2b presents them schematically. Mechanisms A-C correspond to those usually expected for the aminolysis of non-activated esters, which all start with a proton transfer from the N atom but differ in the proton acceptor. The latter can be the water solvent (mechanism A), the negative O^- atom (mechanism B), or the leaving OR group in $T^{\pm}$ (mechanism C). In mechanism A (proton transfer to water), an anionic form of the tetrahedral intermediate (T^-) is formed, which then dissociates to the amide (AM) and to the alkoxide anion (AL^-). Finally, the alkoxide captures a proton from the medium to form the alcohol (AL). Mechanism A parallels that proposed in the experimental study of the PI3Kδ inhibitors.[28] In mechanism B, the proton transfer leads to the formation of a neutral form of the tetrahedral intermediate (T^0), from which the system evolves to the final amide and alcohol products by subsequent proton transfer, from OH to OR group. In mechanism C, the proton transfer to OR leads in a single step to the amide (AM) and alcohol (AL) final products.

In our study, a fourth mechanism, called hereafter mechanism D, has been found in the case of activated phenolic esters. In

contrast to mechanisms A-C, which starts with a proton transfer, mechanism D starts by the heterolytic dissociation of the C-OR bond in the $T^{\pm}$ species forming an ion pair between the N-protonated amide (AM^+) and the leaving alkoxide (AL^-). As the incipient ion pair is being formed, the reaction proceeds (in a more or less concerted way depending on derivative) by the proton transfer between the two moieties, either directly or through water molecules, which allows reaching the amide (AM) and alcohol (AL) products.

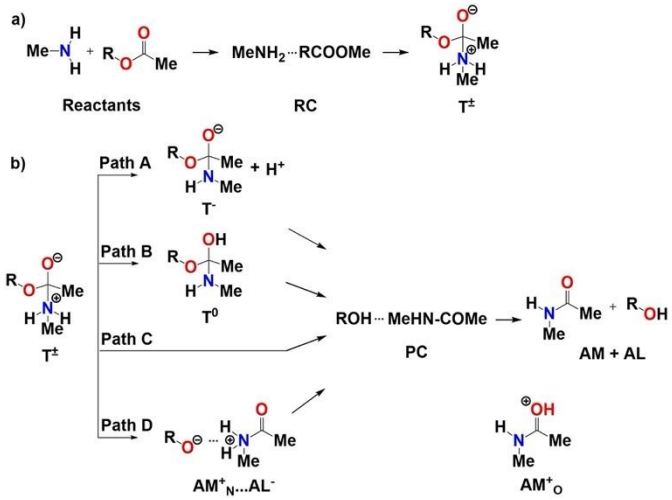

Figure 2. Reaction mechanisms for the ester aminolysis in water solution described in this paper: a) Formation of the pre-reactive complex RC and the zwitterionic tetrahedral intermediate $T^{\pm}$, b) Mechanisms A-D leading from $T^{\pm}$ to the products. R is either the methyl, phenyl or *p*-nitrophenyl group. The following acronyms are used throughout the paper: RC=reactant complex, $T^{\pm}$= zwitterionic tetrahedral intermediate, T^0=neutral tetrahedral intermediate, T^-=anionic intermediate, AM^+_N=N-protonated amide, AM^+_O=O-protonated amide, AL^-=alkoxide intermediate, PC=product complex, AM=amide product, AL=alcohol product. AM^+_O (shown in the bottom right part of the figure) is a structure appearing only in some variants of mechanism B (see text).

The free energy profiles for the studied reaction with MA, PA, and PNPA, are presented in Figures 3-5, respectively. The most relevant structures are drawn in Figures 6-8. The cartesian coordinates of all the systems are provided as supplementary electronic information (Tables S1-S3), as well as the details on the thermodynamic energy calculations (Tables S4-S6), and the imaginary frequency obtained for the transition structures (Table S7). In the description of the mechanisms, we use numbers as subscripts to differentiate between different conformations of a particular structure (e.g. T^0_1, T^0_2, $T^{\pm}_1$, $T^{\pm}_2$, etc.), or between different transition structures (e.g. TS_1, TS_2, etc.). $T^{\pm}_1$ will always represent the tetrahedral intermediate structure reached from RC, while TS(RC-$T^{\pm}_1$) is the transition structure joining them. Note that, in mechanism A, the TS structures for proton transfer to/from bulk water cannot be located in our model, and for this reason, the corresponding reaction paths will be indicated as dashed lines in the Figures below. Likewise, for mechanism B in the case of PA and PNPA, the TSs leading to the formation of PC from ion-pair intermediates could not be located, and dashed lines are used in those cases too. Nevertheless, as shown below, the mechanisms A and B have high barriers in other steps of the overall reaction pathway, and thus can be excluded as favorable mechanisms. For simplicity, TSs structures between different configurations/conformations of the same intermediate or product have not been searched. Note finally that, strictly speaking, in RC (reactant complex) and PC (product complex) there is not always a direct interaction between the ester and amine reagents, or between the amide and alcohol products.

For MA (Figure 3), mechanisms of type A, B and C have been found. Two possibilities have been considered for mechanism A, depending on the location of the proton, first solvation shell or bulk water. In the first case, the ion pair T^-…H_3O^+ can evolve to form the neutral intermediate (T^0_3) and from this point the reaction is like mechanism B. In the second case, the proton has been fully transferred to the bulk and the reaction proceeds through dissociation of the remaining T^- intermediate, forming the amide product (AM) and the alkoxide anion (AL^-), which then captures the proton to form the alcohol (AL). Despite the possible errors introduced by combining MP2 and experimental energies for estimating the stability of the T^- structure (see the methodology section), it seems reasonable to conclude that mechanism A is more likely to occur via T^0_3: this mechanism can be described as a variant of mechanism B in which the proton transfer from N to O^- occurs in a stepwise, water-assisted way. In all mechanisms A, B and C, transition structures displaying high-energy (25 kcal·mol^{-1} or larger) are present somewhere along the reaction paths, suggesting a low reaction rate for the aminolysis of MA, as experimentally found.[65]

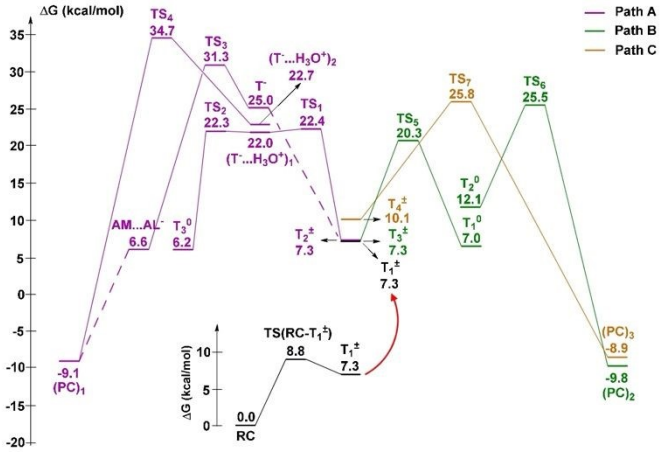

Figure 3. Free energy profile obtained for the methylamine + MA reaction in water at the MP2/aug-cc-pVTZ//B3LYP/6-311+G(d,p) level. For simplicity, the whole reaction path has been separated into two graphs, from RC to $T^{\pm}$, and from $T^{\pm}$ to the products.

The reactions with the activated phenolic esters PA (Figure 4) or PNPA (Figure 5) displays a significantly different landscape compared to MA. Mechanism C joining $T^{\pm}$ to the products directly has not been found in these cases. A variant of Mechanism B has been found for these esters where the dissociation of T^0 to AM…AL is not concerted (as in MA) but proceeds via an ion-pair intermediate (AM^+_O…AL^-) involving the O-protonated amide and the alkoxide. It displays significantly lower activation energies compared to MA. Mechanism A has

also been found, but as for MA, it does not appear to be a favorable pathway. An important result obtained in our study is that the intermediate T^- is not stable for the activated PNPA ester. Indeed, when the zwitterionic tetrahedral intermediate $T^{\pm}$ is deprotonated, the system spontaneously dissociates to form the alkoxide and the amide. A $T^-...H_3O^+$ ion pair intermediate has been located, however.

Mechanism D, which was not found for MA, is a stepwise analog of Mechanism C and appears to be the most favorable pathway for the phenyl derivatives, especially for PNPA. The highest TS in this mechanism lies at about 15 kcal/mol (TS_{14}) for PA and only at about 7.7 kcal/mol (TS_{19}) for PNPA.

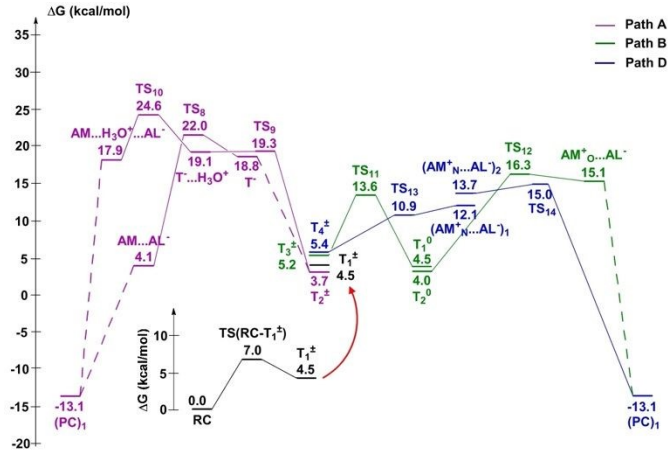

Figure 4. Free energy profile obtained for the methylamine + PA reaction in water at the MP2/aug-cc-pVTZ//B3LYP/6-311+G(d,p) level. For simplicity, the whole reaction path has been separated into two graphs, from RC to $T^{\pm}$, and from $T^{\pm}$ to the products.

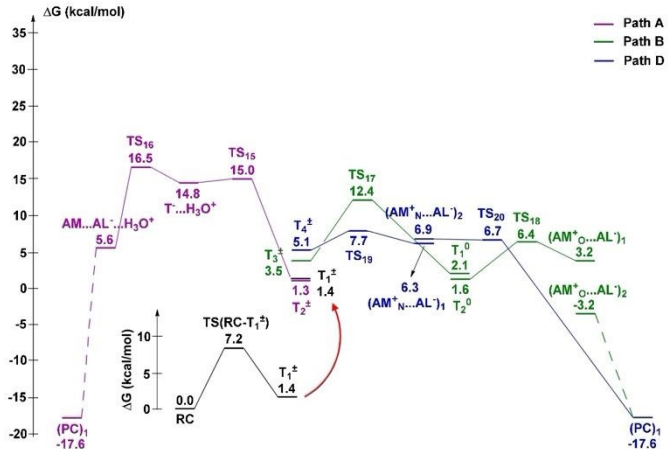

Figure 5. Free energy profile obtained for the methylamine + PNPA reaction in water at the MP2/aug-cc-pVTZ//B3LYP/6-311+G(d,p) level. For simplicity, the whole reaction path has been separated into two graphs, from RC to $T^{\pm}$, and from $T^{\pm}$ to the products.

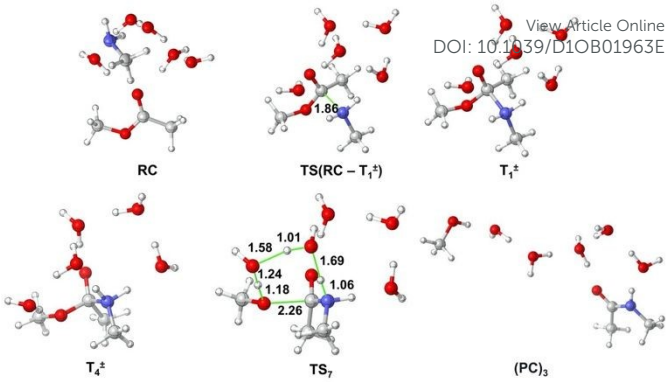

Figure 6. Main stationary structures along path C of MA aminolysis in water optimized at the B3LYP/6-311+G(d,p) level of theory.

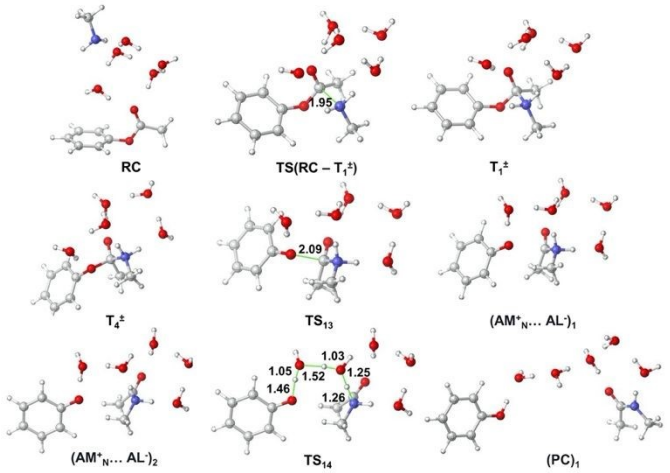

Figure 7. Main stationary structures along path D of PA aminolysis in water optimized at the B3LYP/6-311+G(d,p) level of theory.

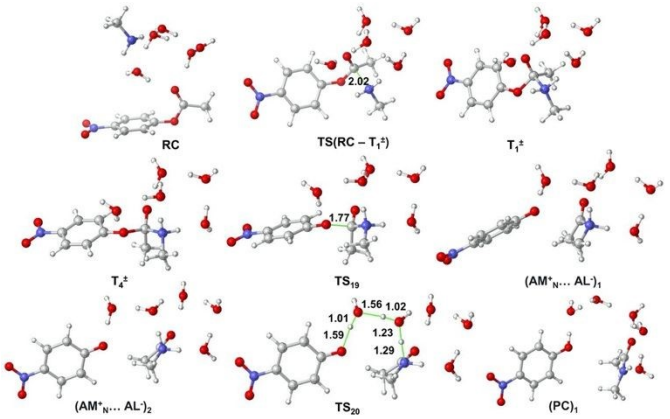

Figure 8. Main stationary structures along path D of PNPA aminolysis in water optimized at the B3LYP/6-311+G(d,p) level of theory..

Figure 9 summarizes and compares the most favorable mechanisms found for the aminolysis of the three esters. For PA and PNPA, mechanism D is the most favorable one, as mentioned. In the case of MA, mechanisms B and C should present a comparable kinetics. We have chosen to represent mechanism C in this Figure since it is the concerted analog of mechanism D. This comparison enlightens several important facts: 1) the aminolysis reaction is considerably faster for the phenyl esters, compared to the alkyl ester, 2) the presence of

the nitro group in the phenyl ring considerably enhances the process, 3) though the same mechanism type holds for PA and PNPA, the bottleneck in the two free energy profiles is different, being final proton transfer for PA (TS_{14}), and zwitterion formation (TS(RC- $T^{\pm}$)) or C-O bond dissociation (TS_{19}) for PNPA, 4) the stability of the zwitterionic intermediates follow the order MA<PA<PNPA, and 5) the reactions are exergonic, with higher reaction energy (in absolute value) in the same order, MA<PA< PNPA.

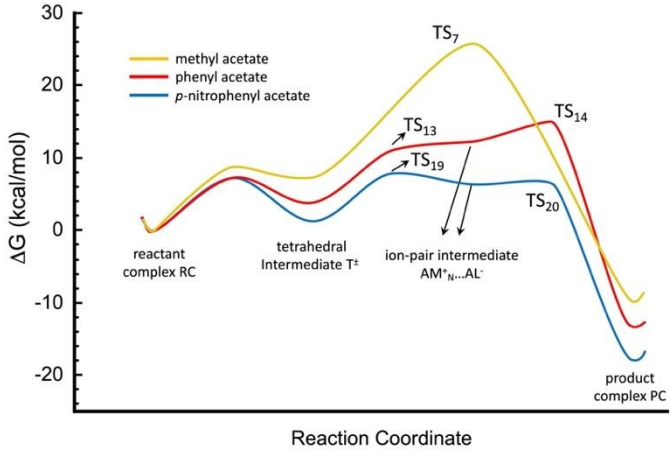

Figure 9. Schematic representation of the most favorable reaction mechanisms for the aminolysis of MA, PA, and PNPA esters in water, as predicted by MP2/aug-cc-pVTZ//B3LYP/6-311+G(d,p) calculations. In this schematic representation, we have systematically considered the most stable conformation/configuration of the reaction intermediates and product complexes.

Experimentally, activated phenolic esters have shown promising properties to be used as PI3Kδ inhibitors, with the *p*-nitrophenyl derivative displaying the most interesting properties among the different esters shown in Scheme 1. Our results, confirming the high reactivity of this ester, explains its strong affinity to covalently bind Lys residues in the enzyme. They also reveal that different reaction mechanisms might be at play for different inhibitors. Mechanisms of type D should be involved in the case of the most efficient covalent inhibitors.

Since mechanism D involves the formation of an alkoxide intermediate, the acidity of the corresponding alcohol is expected to be key in determining the type of the aminolysis reaction pathway. Maude et al[66] have reported an experimental study of the alcohol pK_a influence on aminolysis reactions in acetonitrile, and found that a change of mechanism intervenes at pK_a around 8-9. Our computations confirm a change of mechanism in water too, possibly at a slightly higher pK_a value, since we found different pathways for MA (pK_a=15.2) and PA (pK_a=9.95) or PNPA (pK_a =7.15). Dalton et al[28] tried to relate the inhibitor activity and the alcohol pK_a and reported a subtle relationship. Roughly, they found that K_I is dependent on the leaving group pK_a, while k_{inact} is basically independent. This finding was interpreted as the fact that the zwitterionic intermediate will proceed rapidly to the products in an irreversible way.

To get a deeper insight into the relationship between ester properties and reactivity, we have carried out further computations for the esters in Scheme 2, as models for the inhibitor candidates in Scheme 1. Two main properties have been computed for these esters, namely, the electrophilicity index ω of the ester in gas phase (B3LYP/6-311+G(d,p)) and the free energy difference ΔG between RC and the zwitterionic intermediate $T^{\pm}$ in water (MP2/aug-cc-pVTZ//B3LYP/6-311+G(d,p), same water model as in the calculations presented above). Figure 10 displays the correlations between calculated and experimental properties. Since the experimental k_{inact} appears to be very similar for the different esters, the correlations have been done using the second order rate constant k_{inact}/K_I, which is used to characterize irreversible inhibitors and should capture the global reactivity. As shown in Figure 10, and despite the limited number of available experimental data, we found that the whole set of inhibitor kinetic data and calculated ester properties separate into two different groups corresponding to phenolic derivatives bearing electron-donating (*o,p*-diMePh, *p*-MeOPh) or electron-withdrawing substituents (*p*-FPh, *p*-CF_3Ph, *p*-NO_2Ph), with phenol being in the crossing point. It is worth noting that the correlations of $\ln(k_{inact}/K_I)$ with either ω or ΔG are quite similar, and indeed a comparable correlation is obtained when pK_a is used instead of ω or ΔG (figure not shown), which is not surprising considering the strong interdependency between all these properties. Electron-donating groups usually have lower electrophilicity and higher pK_a compared to electron-withdrawing groups. The split correlation found here (two straight lines intersecting at one point) is quite similar to the correlations found for Maude et al[66] between the measured rate constants of the aminolysis reactions in acetonitrile and the esters pK_a. As in this later case, our study suggests that there is change in mechanism between the phenolic esters bearing electron-donating groups and those carrying electron-withdrawing groups, which strongly increase the inhibition kinetics.

Table 1. Comparison of calculated and experimental properties for selected esters. Calculated electrophilicity index in gas phase ω in eV (B3LYP/6-311+G(d,p) level), zwitterion intermediate formation energy ΔG in kcal/mol (MP2/aug-cc-pVTZ//B3LYP/6-311+G(d,p) level), and experimental pK_a values[67,68] apply for the model esters shown in Scheme 2. Kinetic parameters[28] K_I (M), k_{inact} (s^{-1}) and k_{inact}/K_I ($s^{-1}M^{-1}$) correspond to esters shown in Scheme 1.

R	ω	ΔG	pK_a	K_I	k_{inact}	k_{inact}/K_I
o,p-diMePh	2.10	5.20	10.60	$7.8x10^{-6}$	0.0066	$8.46x10^{2}$
p-MeOPh	2.12	4.67	10.05	$2.2x10^{-6}$	0.0068	$3.09x10^{3}$
Ph	2.36	4.51	9.95	$3.5x10^{-7}$	0.0058	$1.66x10^{4}$
p-FPh	2.65	3.31	9.89	$2.6x10^{-7}$	0.0055	$2.12x10^{4}$
p-CF_3Ph	3.30	3.15	9.39	$2.5x10^{-7}$	0.0070	$2.80x10^{4}$
p-NO_2Ph	5.88	1.38	7.15	$4.0x10^{-8}$	0.0075	$1.88x10^{5}$

View Article Online
DOI: 10.1039/D1OB01963F

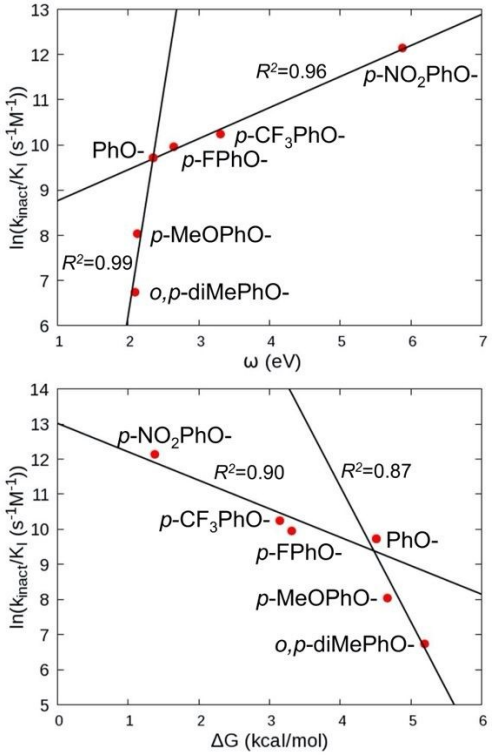

Figure 10. Correlations between calculated and experimental ester properties collected in Table 1 (see the Table for definitions).

Conclusions

The analysis of the different aminolysis pathways of activated phenyl esters studied in our work reveals that the mechanism schematized in Figure 1 for PI3Kδ inhibitors need to be revised. Our calculations indicate that for sufficiently high electrophilic derivatives, such as PNPA, the main reaction coordinate following the formation of the zwitterionic tetrahedral intermediate is not proton transfer, as in mechanism A proposed before for PI3Kδ inhibitors, but C-OR bond dissociation, leading to the formation of an ion pair $AM^+...AL^-$. The development of this important charge separation then provides the driving force for proton transfer and the formation of the final products, which takes place afterwards, along a rather flat free energy surface. This mechanism is in line with previous experimental studies in acetonitrile, which showed that a change of mechanism occurs for leaving groups with a sufficiently low pK_a. Our study indicates that the most efficient inhibitors with phenolic leaving groups should correspond to derivatives bearing electron withdrawing substituents, which activate the ester favoring the formation of the starting zwitterionic intermediate and render the subsequent reaction steps easier. Overall, the experimental inhibitor efficiency has been found to be nicely correlated with the calculated electrophilicity of the ester, and with the stability of the zwitterion. Therefore, the calculation of these properties should be very useful to evaluate a priori the efficacy of other inhibitor candidates.

Obviously, the interactions with the enzymatic environment may modify the mechanisms described here in water solution. Stabilization of the zwitterionic intermediate by electron acceptor residues such as aspartate can be envisaged, which could even be involved in the proton relay process. Future work will focus on the mechanistic aspects of the biological reactions, and the present results provide a very useful framework for exploring them.

Author Contributions

MFRL and SSE designed the research. VF carried out the computations. All authors contributed to analyse data. The manuscript was written through contributions of all authors. All authors have given approval to the final version of the manuscript.

Conflicts of interest

There are no conflicts to declare.

Acknowledgements

The authors thank the French-Turkish PHC Bosphorous program (Project number 44738WL) and TUBITAK (Project number 119N133) for financial support. VF would like to thank the French Ambassy in Turkey for a “co-tutelle” grant. The numerical calculations reported in this paper were partially performed at TUBITAK ULAKBIM, High Performance and Grid Computing Center (TRUBA resources).

Notes and references

1 V. R. Pattabiraman and J. W. Bode, *Nature*, 2011, **480**, 471–479.
2 J. F. Greenberg, Arthur;Breneman, Curt M.; Liebman, *The Amide Linkage: Structural Significance in Chemistry, Biochemistry, and Materials Science*, Wiley-VCH, 2000.
3 A. B. Hughes, *Amino Acids, Peptides and Proteins in Organic Chemistry*, Wiley-VCH, Weinheim, Germany, 2011, vol. 3.
4 P. Knochel and G. A. Molander, *Comprehensive Organic Synthesis: Second Edition*, Elsevier., 2014, vol. 1.
5 S. Kumari, A. V. Carmona, A. K. Tiwari and P. C. Trippier, *J. Med. Chem.*, 2020, **63**, 12290–12358.
6 J. Eckhoff, *Nat. Rev. Chem.*, 2017, **1**, 1–1.
7 E. Massolo, M. Pirola and M. Benaglia, *European J. Org. Chem.*, 2020, **2020**, 4641–4651.
8 K. Marchildon, *Macromol. React. Eng.*, 2011, **5**, 22–54.
9 M. R. Petchey and G. Grogan, *Adv. Synth. Catal.*, 2019, **361**, 3895–3914.
10 T. Krause, S. Baader, B. Erb and L. J. Gooßen, *Nat. Commun.*, 2016, **7**, 1–7.
11 A. Goswami and S. G. Van Lanen, *Mol. Biosyst.*, 2015, **11**, 338–353.
12 K. K. Starheim, K. Gevaert and T. Arnesen, *Trends Biochem. Sci.*, 2012, **37**, 152–161.
13 I. Ali, R. J. Conrad, E. Verdin and M. Ott, *Chem. Rev.*, 2018,

118, 1216–1252.

14 T. A. Baillie, *Angew. Chemie - Int. Ed.*, 2016, **55**, 13408–13421.

15 J. Singh, R. C. Petter, T. A. Baillie and A. Whitty, *Nat. Rev. Drug Discov.*, 2011, **10**, 307–317.

16 J. M. Bradshaw, J. M. McFarland, V. O. Paavilainen, A. Bisconte, D. Tam, V. T. Phan, S. Romanov, D. Finkle, J. Shu, V. Patel, T. Ton, X. Li, D. G. Loughhead, P. A. Nunn, D. E. Karr, M. E. Gerritsen, J. O. Funk, T. D. Owens, E. Verner, K. A. Brameld, R. J. Hill, D. M. Goldstein and J. Taunton, *Nat. Chem. Biol.*, 2015, **11**, 525–531.

17 M. Nacht, L. Qiao, M. P. Sheets, T. St. Martin, M. Labenski, H. Mazdiyasni, R. Karp, Z. Zhu, P. Chaturvedi, D. Bhavsar, D. Niu, W. Westlin, R. C. Petter, A. P. Medikonda and J. Singh, *J. Med. Chem.*, 2013, **56**, 712–721.

18 R. Mah, J. R. Thomas and C. M. Shafer, *Bioorganic Med. Chem. Lett.*, 2014, **24**, 33–39.

19 Q. Liu, Y. Sabnis, Z. Zhao, T. Zhang, S. J. Buhrlage, L. H. Jones and N. S. Gray, *Chem. Biol.*, 2013, **20**, 146–159.

20 F. M. Ferguson and N. S. Gray, *Nat. Rev. Drug Discov.*, 2018, **17**, 353–376.

21 H. Mukherjee and N. P. Grimster, *Curr. Opin. Chem. Biol.*, 2018, **44**, 30–38.

22 L. H. Jones, in *Annual Reports in Medicinal Chemistry*, Academic Press Inc., 2021, vol. 56, pp. 95–134.

23 M. Gehringer, in *Topics in Medicinal Chemistry*, Springer, Berlin, Heidelberg, 2021, vol. 36, pp. 43–94.

24 A. Abdeldayem, Y. S. Raouf, S. N. Constantinescu, R. Moriggl and P. T. Gunning, *Chem. Soc. Rev.*, 2020, **49**, 2617–2687.

25 T. Tamura and I. Hamachi, *J. Am. Chem. Soc.*, 2019, **141**, 2782–2799.

26 R. Liu, Z. Yue, C. C. Tsai and J. Shen, *J. Am. Chem. Soc.*, 2019, **141**, 6553–6560.

27 J. Pettinger, K. Jones and M. D. Cheeseman, *Angew. Chemie - Int. Ed.*, 2017, **56**, 15200–15209.

28 S. E. Dalton, L. Dittus, D. A. Thomas, M. A. Convery, J. Nunes, J. T. Bush, J. P. Evans, T. Werner, M. Bantscheff, J. A. Murphy and S. Campos, *J. Am. Chem. Soc.*, 2018, **140**, 932–939.

29 P. Liu, H. Cheng, T. M. Roberts and J. J. Zhao, *Nat. Rev. Drug Discov.*, 2009, **8**, 627–644.

30 J. R. Somoza, D. Koditek, A. G. Villaseñor, N. Novikov, M. H. Wong, A. Liclican, W. Xing, L. Lagpacan, R. Wang, B. E. Schultz, G. A. Papalia, D. Samuel, L. Lad and M. E. McGrath, *J. Biol. Chem.*, 2015, **290**, 8439–8446.

31 K. Down, A. Amour, I. R. Baldwin, A. W. J. Cooper, A. M. Deakin, L. M. Felton, S. B. Guntrip, C. Hardy, Z. A. Harrison, K. L. Jones, P. Jones, S. E. Keeling, J. Le, S. Livia, F. Lucas, C. J. Lunniss, N. J. Parr, E. Robinson, P. Rowland, S. Smith, D. A. Thomas, G. Vitulli, Y. Washio and J. N. Hamblin, *J. Med. Chem.*, 2015, **58**, 7381–7399.

32 H. Zipse, L.-H. Wang and K. N. Houk, *Liebigs Ann.*, 1996, **1996**, 1511–1522.

33 L. H. Wang and H. Zipse, *Liebigs Ann.*, 1996, **1996**, 1501–1509.

34 G. Q. Yi, Y. Zeng, X. F. Xia, Y. Xue, C. K. Kim and G. Sen Yan, *Chem. Phys.*, 2008, **345**, 73–81.

35 B. Galabov, S. Ilieva, B. Hadjieva, Y. Atanasov and H. F. Schaefer, *J. Phys. Chem. A*, 2008, **112**, 6700–6707.

36 H. B. Rao, Y. Y. Wang, X. Y. Zeng, Y. Xue and Z. R. Li, *Comput. Theor. Chem.*, 2013, **1008**, 8–14.

37 D. Suárez and K. M. Merz, *J. Am. Chem. Soc.*, 2001, **123**, 7687–7690.

38 W. Yang and D. G. Drueckhammer, *Org. Lett.*, 2000, **2**, 4133–4136.

39 D. A. Singleton and S. R. Merrigan, *J. Am. Chem. Soc.*, 2000, **122**, 11035–11036.

40 S. Chalmet, W. Harb and M. F. Ruiz-López, *J. Phys. Chem. A*, 2001, **105**, 11574–11581.

41 B. Galabov, Y. Atanasov, S. Ilieva and H. F. Schaefer, *J. Phys. Chem. A*, 2005, **109**, 11470–11474.

42 S. Ilieva, B. Galabov, D. G. Musaev, K. Morokuma and H. F. Schaefer, *J. Org. Chem.*, 2003, **68**, 1496–1502.

43 X. Xia, C. Zhang, Y. Xue, C. K. Kim and G. Yan, *J. Chem. Theory Comput.*, 2008, **4**, 1643–1653.

44 D. D. Sung, I. S. Koo, K. Yang and I. Lee, *Chem. Phys. Lett.*, 2006, **426**, 280–284.

45 S. Ilieva, Y. Atanasov and B. Galabov, *Bulg. Chem. Commun.*, 2008, **40**, 401–408.

46 D. Rajarathnam, T. Jeyakumar and P. A. Nadar, *Int. J. Chem. Kinet.*, 2005, **37**, 211–221.

47 D. Rajarathnam, T. Jeyakumar and P. A. Nadar, *Int. J. Chem. Kinet.*, 2002, **34**, 366–373.

48 G. M. Blackburn and W. P. Jencks, *J. Am. Chem. Soc.*, 1968, **90**, 2638–2645.

49 A. Arcelli and C. Concilio, *J. Org. Chem.*, 1996, **61**, 1682–1688.

50 E. A. Castro, D. Millan, R. Aguayo, P. R. Campodónico and J. G. Santos, *Int. J. Chem. Kinet.*, 2011, **43**, 687–693.

51 J. F. Marlier, B. A. Haptonstall, A. J. Johnson and K. A. Sacksteder, *J. Am. Chem. Soc.*, 1997, **119**, 8838–8842.

52 L. Gorb, A. Asensio, I. Tuñón and M. F. Ruiz-López, *Chem. - A Eur. J.*, 2005, **11**, 6743–6753.

53 R. Montecinos, M. Gazitúa and J. G. Santos, *New J. Chem.*, 2019, **43**, 6372–6379.

54 R. Montecinos, M. E. Aliaga, P. Pavez and J. G. Santos, *New J. Chem.*, 2017, **41**, 9954–9962.

55 L. Jin, Y. Wu, Y. Xue, Y. Guo, D. Q. Xie and G. Sen Yan, *Acta Chim. Sin.*, 2006, **64**, 873–878.

56 S. Chalmet, W. Harb and M. F. Ruiz-López, *J. Phys. Chem. A*, 2001, **105**, 11574–11581.

57 K. Fukui, *Acc. Chem. Res.*, 1981, **14**, 363–368.

58 T. Yanai, D. P. Tew and N. C. Handy, *Chem. Phys. Lett.*, 2004, **393**, 51–57.

59 M. Head-Gordon, J. A. Pople and M. J. Frisch, *Chem. Phys. Lett.*, 1988, **153**, 503–506.

60 N. Derbel, I. Clarot, M. Mourer, J. B. Regnouf-De-Vains and M. F. Ruiz-López, *J. Phys. Chem. A*, 2012, **116**, 9404–9411.

61 P. Geerlings, F. De Proft and W. Langenaeker, *Chem. Rev.*, 2003, **103**, 1793–1873.

62 M. J. Frisch, G. W. Trucks, H. B. Schlegel, G. E. Scuseria, M. A. Robb, J. R. Cheeseman, G. Scalmani, V. Barone, B. Mennucci, G. A. Petersson and E. Al., 2009.

View Article Online
DOI: 10.1039/D1OB01963E

63 S. Chalmet, W. Harb and M. F. Ruiz-López, *J. Phys. Chem. A*, 2001, **105**, 11574–11581.
64 T. C. Bruice and M. F. Mayahi, *J. Am. Chem. Soc.*, 1960, **82**, 3067–3071.
65 A. C. Satterthwait and W. P. Jencks, *J. Am. Chem. Soc.*, 1974, **96**, 7018–7031.
66 A. B. Maude and A. Williams, *J. Chem. Soc. Perkin Trans. 2*, 1997, 179–183.
67 E. P. Serjeant and B. Dempsey, *Ionisation Constants of Organic Acids in Aqueous Solution*, Pergamon Press, New York, 1979, vol. 23.
68 B. Slater, A. McCormack, A. Avdeef and J. E. A. Comer, *J. Pharm. Sci.*, 1994, **83**, 1280–1283.